Possible multiple chiral doublet bands in odd-odd ^{128}La

J. X. Teng (滕佳欣),[1] K. Y. Ma (马克岩),[1,2,3,*] J. B. Lu (陆景彬),[1,†] H. C. Zhang (张会成),[1] H. Wang (王豪),[1] S. Y. Liu (刘斯颖),[1] D. Zhao (赵迪),[1] H. Y. Ye (叶欢仪),[1] J. Y. Li (李纪元),[1] X. J. Zhao (赵新洁),[1] Z. H. Zhao (赵子豪),[1] Y. C. Hao (郝宜春),[1] Z. Qiao (乔政),[1] Y. J. Ma (马英君),[1] D. Yang (杨东),[1] X. G. Wu (吴晓光),[4] Y. Zheng (郑云),[4] and C. B. Li (李聪博)[4]

[1]*College of Physics, Jilin University, Changchun 130012, China*
[2]*Chongqing Research Institute, Jilin University, Chongqing 401120, China*
[3]*Yibin Research Institute, Jilin University, Sichuan 644000, China*
[4]*China Institute of Atomic Energy, Beijing 102413, China*

(Received 22 October 2023; accepted 27 February 2024; published 13 March 2024)

High-spin states of ^{128}La have been populated by the ^{118}Sn(^{14}N, $4n$) ^{128}La reaction at a beam energy of 69 MeV. The previously known level scheme of ^{128}La is extended with the addition of 27 γ transitions. A new negative-parity band with the same $\pi h_{11/2} \otimes \nu d_{5/2}$ configuration as that of the yrare band is observed in ^{128}La. This pair of negative-parity bands is suggested to be candidate chiral doublet bands, which is supported by the particle rotor model calculations. Meanwhile, the newly identified negative-parity chiral doublet bands together with the previously known pair of positive-parity chiral doublet bands constitute a case of multiple chiral doublet bands in the odd-odd nucleus ^{128}La. Furthermore, systematic studies of multiple chiral doublet bands are presented in this work.

DOI: 10.1103/PhysRevC.109.034308

I. INTRODUCTION

Chirality is well known in branches of science like nuclear physics, molecular physics, chemistry, biology, etc. In nuclear physics, chirality has attracted significant attention both experimentally and theoretically over the past two decades since it was first predicted by Frauendorf and Meng in 1997 [1]. They point out that, in the laboratory frame, the restoration of the broken chiral symmetry may result in pairs of nearly degenerate $\triangle I = 1$ bands with the same parity, i.e., chiral doublet bands. Theoretically, chiral doublet bands have been successfully denoted by the particle rotor model (PRM) [2–8], the tilted axis cranking approach [9–13], the random-phase approximation [14], the angular momentum projection method [15,16], the interacting boson-fermion model [17,18], the collective Hamiltonian method [19,20], the critical point symmetries method [21], etc. Experimentally, about 50 chiral nuclei have been reported in the $A \approx 80$, 110, 130, and 190 mass regions [22–30].

In most chiral nuclei, only one pair of chiral doublet bands is observed, but in a few chiral nuclei, two or more pairs of chiral doublet bands are identified, exhibiting an exotic phenomenon of multiple chiral doublet (MχD) bands. Up to now, the MχD bands have been reported in ^{78}Br [31], ^{81}Kr [32], ^{103,105}Rh [33–35], ^{107}Ag [36,37], ^{131}Ba [38], ^{133}Ce [39], ^{135,136,137}Nd [40–44], and ^{195}Tl [45]. As mentioned above, the reported MχD bands predominantly exist in odd-A and even-even nuclei, while the experimental study of MχD bands in the odd-odd isotopes is very scarce; i.e., only one case has been identified in odd-odd ^{78}Br nucleus in the $A \approx 80$ mass region. Thus, it is interesting to look for more examples of MχD bands and examine their chiral manifestations in the odd-odd nucleus. For this purpose, the $A \approx 130$ mass region, in which the first chiral doublet bands are reported, seems to be a good candidate. Additionally, the largest island of chiral rotation is suggested in the $A \approx 130$ mass region, where a number of MχD bands have been proposed in odd-A and even-even nuclei, except odd-odd nuclei. Hence, it is also necessary to explore the existence of possible MχD bands in the odd-odd nucleus in this mass region.

Prior to this work, we have reported a pair of chiral doublet bands based on the $\pi h_{11/2} \otimes \nu h_{11/2}$ configuration in the odd-odd nucleus ^{128}La 11 years ago [46]. Since then, our effort to further study ^{128}La nuclei has not been interrupted. In this paper, another pair of near-degenerate doublet bands with the configuration of $\pi h_{11/2} \otimes \nu d_{5/2}$ is identified in ^{128}La, suggesting that MχD bands are likely to exist in a single odd-odd nucleus in the $A \approx 130$ mass region. This is also the first example of MχD bands in an odd-odd nucleus in this mass region. The relevant details of chiral rotation are discussed in Sec. IV.

II. EXPERIMENTAL DETAILS

Excited states of ^{128}La have been populated following the ^{118}Sn(^{14}N, $4n$) reaction at a beam energy of 69 MeV. The beam is provided by the HI-13 tandem accelerator at China Institute of Atomic Energy in Beijing. The tin target consists of 2.4 mg/cm^2 of ^{118}Sn (92.8% enrichment) rolled onto a lead backing of thickness 19 mg/cm^2, with the lead backing sufficient to stop the recoils in order to reduce Doppler broadening

*mky@jlu.edu.cn
†ljb@jlu.edu.cn

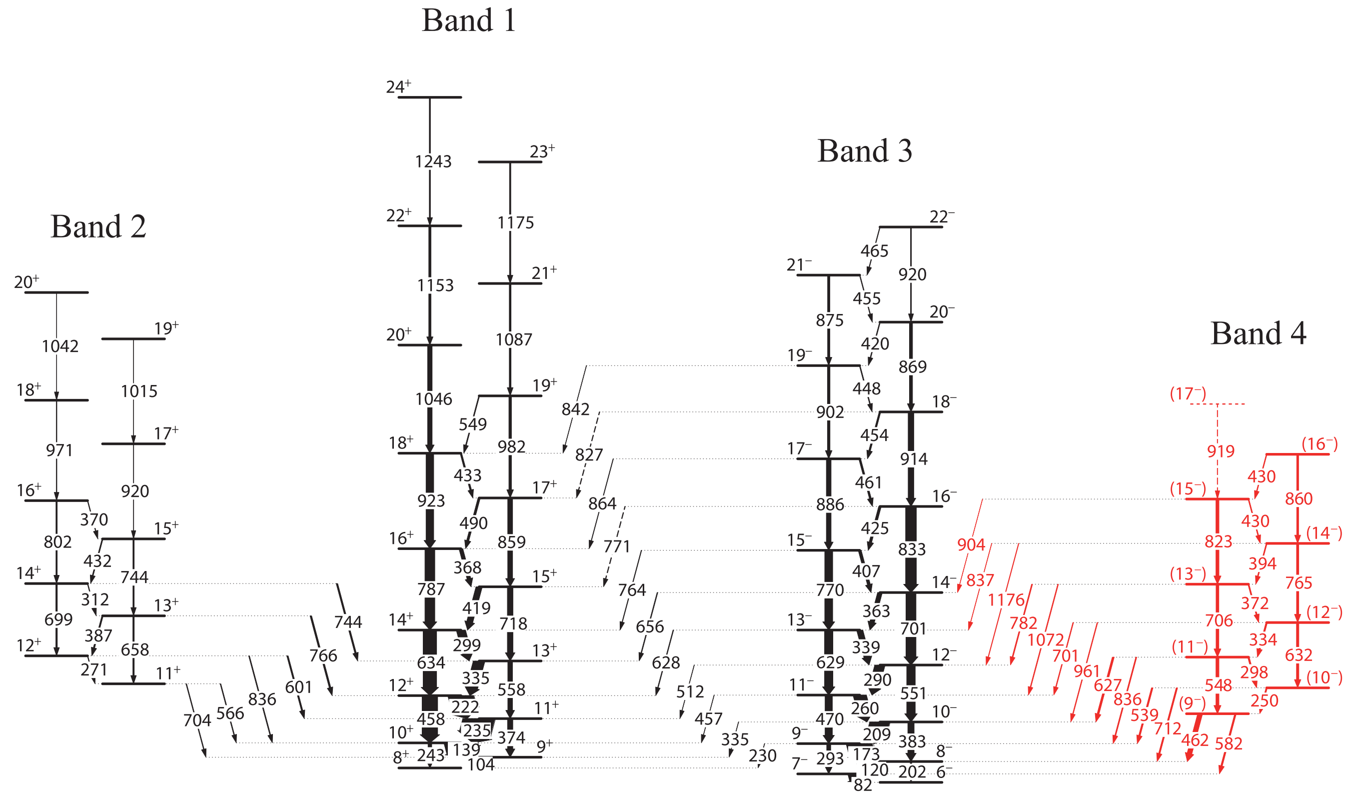

FIG. 1. Partial level scheme of ^{128}La deduced from the present work. Transition energies are given in keV and their measured relative intensities are proportional to the widths of the arrows. The new transitions and levels are indicated in red.

of the low-energy γ rays of interest. The detecting system consists of 14 Compton-suppressed high-purity germanium (HPGe) detectors and 2 HPGe planar detectors. A total of 3.6×10^8 γ-γ coincidence events are collected in this experiment. The data are sorted into a symmetrized γ-γ coincidence matrix and a directional correlation ratios of oriented states (DCO) matrix. In the present detector array geometry, when gating on a stretched quadrupole transition, the DCO ratio of the measured transition is around 1 for a stretched quadrupole transition and around 0.6 for a dipole transition, and when gating on a dipole transition, the DCO ratio of the measured transition becomes around 1 for a dipole transition and around 1.7 for a stretched quadrupole transition.

III. RESULTS

A partial level scheme of ^{128}La derived from the present work is shown in Fig. 1, where bands 1 and 3 have been previously reported by Godfrey *et al.* [47,48] and Hayakawa *et al.* [49]. Subsequently, band 2 has also been observed, and it is interpreted as the partner band of the candidate chiral doublet bands in our early work [46]. Band 4 is a new band deduced from the present experiment. The current study extends this band up to the $I^\pi = (17^-)$ state, and 13 new linking transitions between bands 3 and 4 are observed. A total of 27 new transitions and 9 new levels are added to the level scheme of ^{128}La. Figure 2 shows the γ-ray coincidence spectrum, which supports the existence of band 4. The newly observed γ rays and their energies, intensities, DCO ratios, and multipolarities are listed in Table I.

Band 4 decays predominantly to band 3 via multiple paths, which unambiguously determines the excitation energies of band 4. Multipolarity analysis indicates that the 712- and 836-keV linking transitions are of $\Delta I = 2$ character with DCO ratios of 1.76(58) and 1.59(57), respectively, and the 462- and 539-keV linking transitions are of $\Delta I = 1$ character with DCO ratios of 1.04(19) and 1.16(39), respectively (DCO

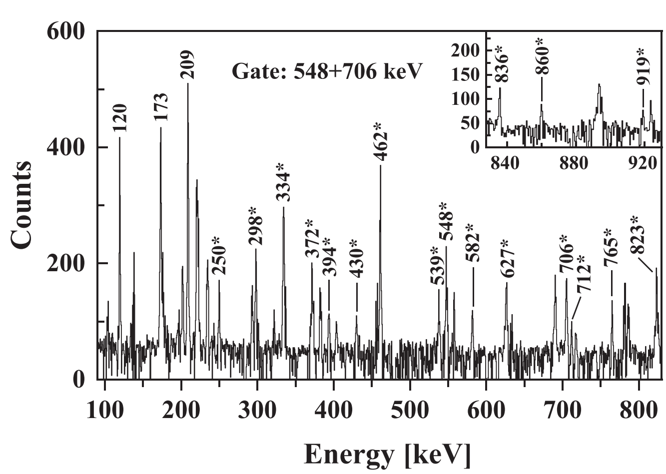

FIG. 2. A spectrum of γ rays gated on a sum of 548- and 706-keV transitions. Asterisks are used to indicate the newly identified rays.

TABLE I. Energies, intensities, and DCO ratios for new transitions assigned to ^{128}La in the present work.

E_γ [a] (keV)	I_γ [b]	E_γ [c] (keV)	R_{DCO}	$I_i^\pi - I_f^\pi$	Multipolarity
Band 4					
250.1	4.2	119.7	1.13(39)	$(10^-) \longrightarrow (9^-)$	$(M1/E2)$
297.6	4.9	173.3	0.97(32)	$(11^-) \longrightarrow (10^-)$	$(M1/E2)$
334.1	4.7	209.2	1.09(36)	$(12^-) \longrightarrow (11^-)$	$(M1/E2)$
371.6	3.8	260.2	1.11(40)	$(13^-) \longrightarrow (12^-)$	$(M1/E2)$
393.7	3.1	260.2	1.12(41)	$(14^-) \longrightarrow (13^-)$	$(M1/E2)$
429.6	2.9			$(15^-) \longrightarrow (14^-)$	$(M1/E2)$
430.4	2.5			$(16^-) \longrightarrow (15^-)$	$(M1/E2)$
547.7	9.8	119.7	1.79(57)	$(11^-) \longrightarrow (9^-)$	$(E2)$
631.8	7.8	173.3	1.75(57)	$(12^-) \longrightarrow (10^-)$	$(E2)$
705.8	9.1	209.2	1.64(53)	$(13^-) \longrightarrow (11^-)$	$(E2)$
765.4	7.3	260.2	1.82(60)	$(14^-) \longrightarrow (12^-)$	$(E2)$
823.2	9.9	290.4	1.84(58)	$(15^-) \longrightarrow (13^-)$	$(E2)$
860.1	6.3	290.4	1.64(54)	$(16^-) \longrightarrow (14^-)$	$(E2)$
919.3	1.5			$(17^-) \longrightarrow (15^-)$	$(E2)$
Linking γ rays between bands 3 and 4					
461.8	15.4	119.7	1.04(19)	$(9^-) \longrightarrow 8^-$	$(M1/E2)$
538.5	4.9	173.3	1.16(39)	$(10^-) \longrightarrow 9^-$	$(M1/E2)$
581.6	5.0	81.8	1.87(64)	$(9^-) \longrightarrow 7^-$	$(E2)$
627.0	6.2	209.2	1.07(44)	$(11^-) \longrightarrow 10^-$	$(M1/E2)$
700.9	2.4			$(12^-) \longrightarrow 11^-$	$(M1/E2)$
711.9	4.5	119.7	1.76(58)	$(10^-) \longrightarrow 8^-$	$(E2)$
782.1	3.2	290.4	1.18(43)	$(13^-) \longrightarrow 12^-$	$(M1/E2)$
836.2	3.3	173.3	1.59(57)	$(11^-) \longrightarrow 9^-$	$(E2)$
837.4	1.0			$(14^-) \longrightarrow 13^-$	$(M1/E2)$
904.3	0.8			$(15^-) \longrightarrow 14^-$	$(M1/E2)$
961.1	2.3			$(12^-) \longrightarrow 10^-$	$(E2)$
1072.4	2.5			$(13^-) \longrightarrow 11^-$	$(E2)$
1175.7	1.6			$(14^-) \longrightarrow 12^-$	$(E2)$

[a] The energy uncertainty is about 0.2 keV for strong transitions and about 0.5 keV for weak transitions.
[b] An intensity set to 100 for the 235-keV transition in Band 1 [46]. Uncertainties on the relative intensities vary from ≈ 10% for strong transitions ($I_\gamma \geqslant 10$) up to ≈ 30% for weak transitions ($I_\gamma < 10$).
[c] Using the $M1$ transitions as gates.

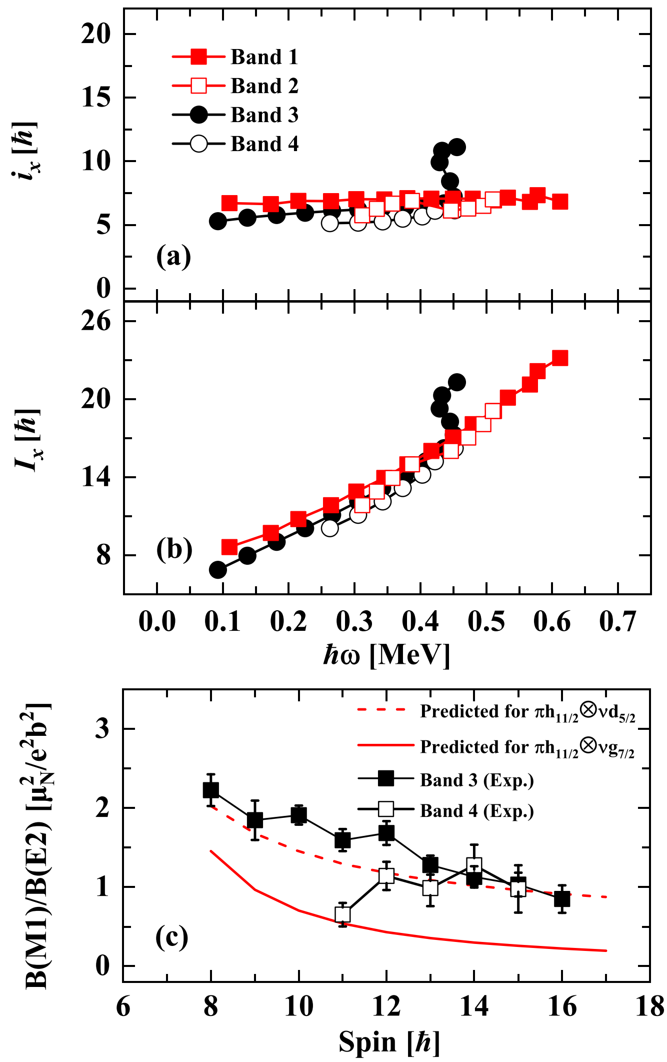

FIG. 3. (a) Aligned angular momenta as a function of rotational frequency for the bands 1–4 in ^{128}La. The Harris parameters are adopted as $J_0 = 17$ MeV^{-1} $\hbar^2$ and $J_1 = 25.8$ MeV^{-3} $\hbar^4$. (b) Total aligned angular momenta ($I_x = [I(I+1) - K^2]^{1/2}$) as a function of rotational frequency for the bands 1–4 in ^{128}La. (c) Comparison of experimental and predicted $B(M1)/B(E2)$ values for bands 3 and 4 in the geometrical model.

ratios from gating on the dipole transitions). The observation of both $\Delta I = 1$ and $\Delta I = 2$ linking transitions between bands 3 and 4 implies that band 4 has the same negative parity as that of band 3. In addition, several new $E2$ crossover transitions of 548, 632, 706, 765, 823, 860, and 919 keV are observed, thereby confirming the ordering of the dipole transitions of band 4 up to the $I^\pi = (17^-)$ level.

IV. DISCUSSION

Band 3 assigned as the $\pi h_{11/2} \otimes \nu d_{5/2}$ configuration has been reported in Ref. [50]. The newly observed negative-parity band 4 decays to band 3 via several dipole and quadrupole transitions. As shown in Fig. 1, band 4 has the same negative parity as band 3. The existence of several $M1/E2$ and $E2$ linking transitions between bands 3 and 4 indicates that these two bands possibly have similar matrix elements [51–53], and bands 3 and 4 exhibit almost the same initial alignment $i_x \approx 6\hbar$ in Fig. 3(a), suggesting that band 4 possibly has the same intrinsic configuration as that of band 3. It is worth mentioning that the chiral partner bands built on the identical $\pi h_{11/2} \otimes \nu h_{11/2}$ configuration in odd-odd Cs, La, Pr, and Pm isotopes in the $A \approx 130$ mass region also systematically display similar alignment behavior. For example, the partner bands 1 and 2 of ^{128}La are shown in Fig. 3(a), and the partner bands are reported in neighboring nuclei ^{126,128}Cs and ^{130,132}La [54,55]. Furthermore, the total aligned angular momenta I_x as a function of rotational frequency ω for the bands 1–4 are presented in Fig. 3(b), where band 3 with the configuration of $\pi h_{11/2} \otimes \nu d_{5/2}$ exhibits a sharp backbend at $\hbar\omega \approx 0.45$ MeV attributed to the rotational alignment of the first pair of $h_{11/2}$ neutrons [47]. Below the crossing frequency, the I_x curves for bands 3 and 4 exhibit similar behavior, indicating that band 4 is also built on a two-particle configuration like

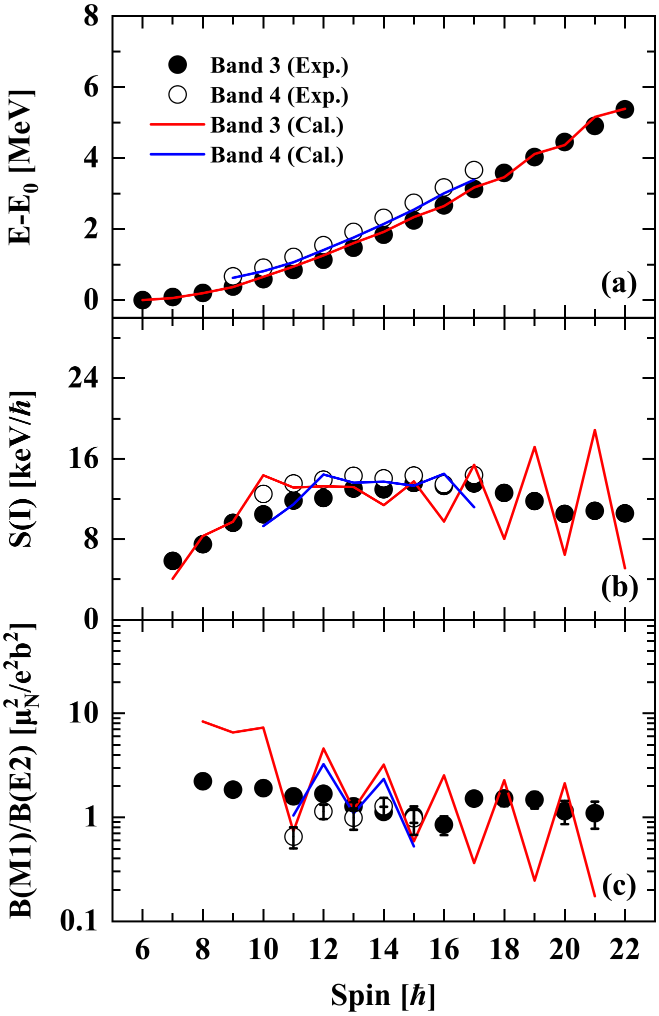

FIG. 4. Experimental excitation energies, energy staggering parameters $S(I)$, and $B(M1)/B(E2)$ ratios for the negative-parity doublet bands in ^{128}La as a function of spin in comparison with the PRM calculations. The deformation parameter $\beta = 0.25$ [47] and the triaxial deformation parameter $\gamma = 24.5^{\circ}$ are adopted as input to the PRM. The energies are relative to the bandhead E_0 of the chiral double bands.

that of band 3. For bands 1 and 2, no crossing is observed below 0.6 MeV in Fig. 3(b), which implies that the $\nu h_{11/2}$ orbital is Pauli blocked in both bands. Hence, a $\nu h_{11/2}$ orbital should be involved in the configurations of bands 1 and 2, supporting the previous configuration assignment of the two bands [46].

In order to further verify the configuration for the newly observed band 4, the experimental $B(M1)/B(E2)$ ratios of bands 3 and 4 together with theoretical estimates based on the geometrical model [56] are plotted in Fig. 3(c), in which the calculated results using the $\pi h_{11/2} \otimes \nu d_{5/2}$ configuration are in good agreement with the experimental values of bands 3 and 4, while those using the $\pi h_{11/2} \otimes \nu g_{7/2}$ configuration deviate significantly from the experimental data, thereby inferring that these two bands are probably based on predominantly the $d_{5/2}$ neutron. Even so, an alternative interpretation that bands 3 and 4 are built on a mixed $d_{5/2}$ and $g_{7/2}$ valence neutron configuration could not be ruled out completely.

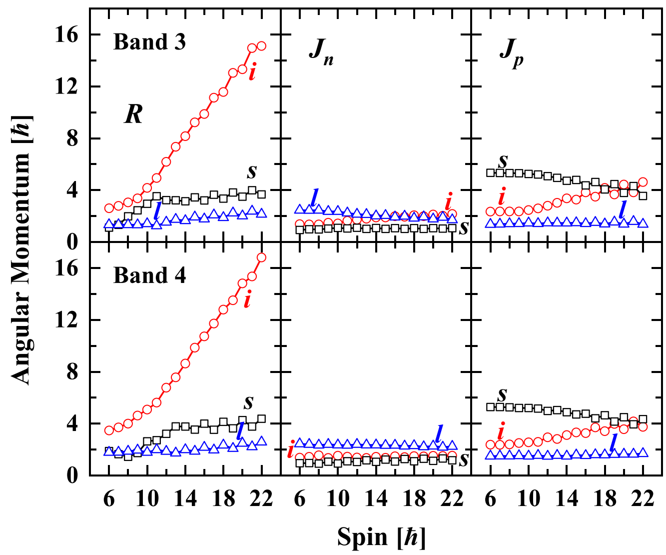

FIG. 5. The root-mean-square components along the intermediate (i, circles), short (s, squares), and long (l, triangles) axes of the core, valence neutron, and valence proton angular momenta calculated as functions of spin I by means of the PRM for the doublet bands in ^{128}La.

Considering the fact that bands 3 and 4 with the same configuration are close to each other in energy, we speculate that band 4 might be a chiral partner band of band 3. To investigate the properties of bands 3 and 4, the excitation energies $E(I)$, the energy staggering parameters $S(I) = [E(I) - E(I-1)]/2I$, and the $B(M1)/B(E2)$ ratios are extracted and presented in Fig. 4 as functions of spin. As shown in Fig. 4(a), the excitation energy curve of band 4 is slightly higher than that of band 3, and the two bands show a small energy difference within the observed spin range. In Fig. 4(b), the doublet bands have similar $S(I)$ values and exhibit smooth variation of $S(I)$ with increasing spin. Moreover, the $B(M1)/B(E2)$ ratios for bands 3 and 4 show odd-even staggering with the same phase as a function of spin in Fig. 4(c). These experimental properties are consistent with the fingerprints of chiral doublet bands [3,57–59]. Hence, the negative-parity bands 3 and 4 of ^{128}La are suggested as a pair of candidate chiral doublet bands with the $\pi h_{11/2} \otimes \nu d_{5/2}$ configuration.

To further examine the existence of possible chirality in bands 3 and 4, we have carried out the calculations based on the PRM. The calculated $E(I)$ and $S(I)$ and the $B(M1)/B(E2)$ ratios for the doublet bands with the $\pi h_{11/2} \otimes \nu d_{5/2}$ configuration in ^{128}La are shown in comparison with the corresponding experimental results in Fig. 4. It can be seen that the calculated $E(I)$ values are in good agreement with the experimental data and $S(I)$ values are generally reproduced for bands 3 and 4. In addition, the staggering phase of the calculated $B(M1)/B(E2)$ ratio in band 3 is the same as that of band 4, which reproduces the experimental staggering and the trend pattern. The agreement between the experiments and the theoretical calculations supports the present configuration assignment and allows us to investigate the chiral geometry for bands 3 and 4 in ^{128}La.

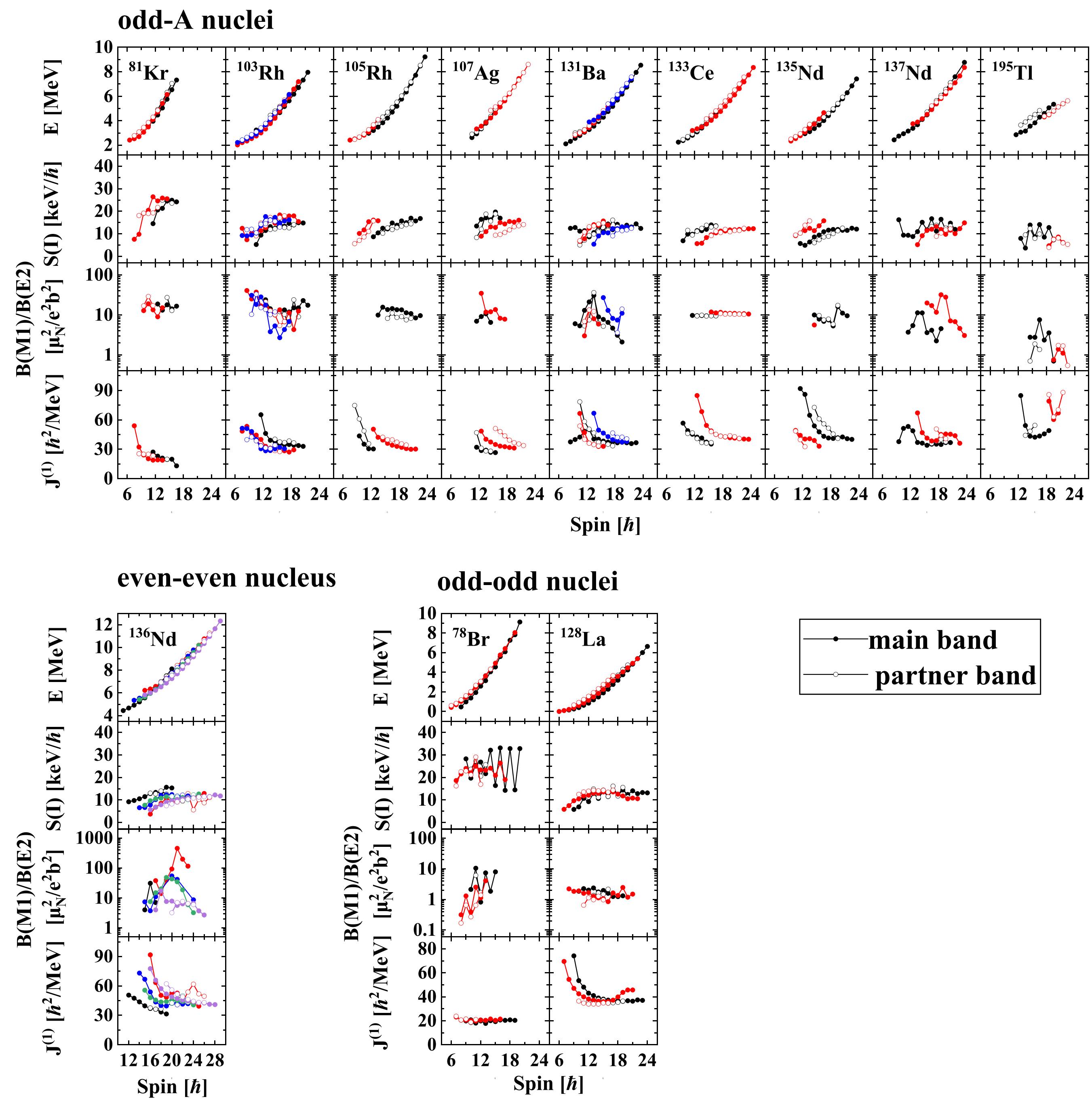

FIG. 6. The excitation energies $E(I)$, the energy staggering parameters $S(I)$, the $B(M1)/B(E2)$ ratios, and the kinematic moments of inertia $J^{(1)}$ as a function of spin for MχD bands. The solid and open symbols correspond to the main band and the partner band, respectively.

In order to exhibit the chiral geometry in ^{128}La, the root-mean-square values of the angular momentum components for the core $R_k = \sqrt{\langle \hat{R}_k^2 \rangle}$, the valence neutron $J_{nk} = \sqrt{\langle \hat{j}_{nk}^2 \rangle}$, and the valence proton $J_{pk} = \sqrt{\langle \hat{j}_{pk}^2 \rangle}$ along three principal axes for bands 3 and 4 are calculated as presented in Fig. 5, in which $k = i$, s, and l represent the intermediate, short, and long axes, respectively. It is clear that the core angular momentum mainly aligns along the intermediate axis. Meanwhile, the angular momentum of the valence neutron $d_{5/2}$ and the valence proton $h_{11/2}$ mainly align along the long axis and the short axis, respectively. The chiral geometry of bands 3 and 4 supports the existence of possible chiral doublet bands in ^{128}La. The newly identified negative-parity chiral doublet bands together with the previously known pair of positive-parity chiral doublet bands constitute a case of multiple chiral doublet (MχD) bands in the odd-odd nucleus ^{128}La. Moreover, it is worth noting that band 3 decays to band 1 through several $E1$ transitions, and a similar situation has also been systematically observed in the neighboring odd-odd nuclei ^{124}La [60], ^{124}Cs [61], and ^{122}Cs [62]. The observation of the $E1$ transitions between positive-parity band 1 and negative-parity band 3 implies the possible existence of the octupole correlations in ^{128}La. The configurations of bands 1 and 3 are currently interpreted as $\pi h_{11/2} \otimes \nu h_{11/2}$ and $\pi h_{11/2} \otimes \nu d_{5/2}$, respectively. The only difference between two such configurations is that one of the two particles occupies the $\nu h_{11/2}$ single-particle orbital in band 1, whereas the other occupies the $\nu d_{5/2}$ single-particle orbital in band 3. The interaction between $\nu h_{11/2}$ and $\nu d_{5/2}$ orbitals with opposite parities and $\Delta j = \Delta l = 3\hbar$ might lead to the octupole correlations in ^{128}La.

From the above discussions, ^{128}La is proposed to be a candidate multiple chiral nucleus. The excitation energies $E(I)$, the energy staggering parameters $S(I)$, the $B(M1)/B(E2)$ ratios, and the kinematic moments of inertia $J^{(1)}$ for MχD bands in ^{128}La are shown in Fig. 6 in comparison with the currently known 11 multiple chiral nuclei. It is clear from Fig. 6 that $E(I)$, $S(I)$, $B(M1)/B(E2)$, and $J^{(1)}$ of ^{128}La and other multiple chiral nuclei are generally in agreement with the properties of MχD bands.

In addition, a few interesting phenomena are also exhibited in Fig. 6. First, there is an energy crossing of chiral doublet bands in ^{105}Rh [35], ^{107}Ag [36,37], and ^{136}Nd [42,43]. Besides, the MχD bands concentrate in the odd-Z nuclei ^{103,105}Rh [33–35] and ^{107}Ag [36,37] in the $A \approx 100$ mass region, where the chiral doublet bands in these nuclei have been assigned the $\pi g_{9/2} \otimes \nu h^2_{11/2}$ and $\pi g_{9/2} \otimes \nu h_{11/2}(g_{7/2}/d_{5/2})$ configurations, respectively. However, in the $A \approx 130$ mass region, the MχD bands mainly exist in the odd-N nuclei ^{131}Ba [38], ^{133}Ce [39], and ^{135,137}Nd [40,41,44], in which the configurations of chiral doublet bands are interpreted as $\pi h_{11/2} g_{7/2} \otimes \nu h_{11/2}$ and $\pi h^2_{11/2} \otimes \nu h_{11/2}$, respectively. It is worthwhile to mention here the existence of two chiral doublet bands with the same configuration built on $\pi g_{9/2} \otimes \nu h_{11/2}(g_{7/2}/d_{5/2})$ in ^{103}Rh [33]. A similar phenomenon built on the $\pi h_{11/2} g_{7/2} \otimes \nu h_{11/2}$ configuration is also observed in ^{131}Ba [38]. In addition, the pseudospin-chiral triplet bands and pseudospin-chiral quartet bands have been reported in ^{81}Kr [32] and ^{131}Ba [38], respectively. For even-even nuclei, the MχD bands have been observed only in ^{136}Nd [42,43], which has five pairs of chiral doublet bands. For odd-odd nuclei, the first MχD bands are suggested to be in ^{78}Br [31]. Meanwhile, the octupole correlations are also observed in this nucleus. Coincidentally, the coexistence of MχD bands and octupole correlations also occurs in the odd-odd nucleus ^{128}La.

V. SUMMARY

Excited states of ^{128}La have been studied by using the ^{118}Sn(^{14}N, $4n$) reaction at a beam energy of 69 MeV. A total of 27 new transitions and 9 new levels are added to the level scheme of ^{128}La compared with the previous work. A negative-parity rotational band assigned to the same $\pi h_{11/2} \otimes \nu d_{5/2}$ configuration as that of the yrare band is observed for the first time in ^{128}La. The experiment excitation energies $E(I)$, the energy staggering parameters $S(I)$, and the $B(M1)/B(E2)$ ratios of the pair of negative-parity bands are consistent with the fingerprints of chiral rotation. Thus, the negative-parity doublet bands are interpreted as candidate chiral doublet bands. The PRM calculations reproduce the experimental results well and support this interpretation. Furthermore, the observation of the new chiral doublet bands with the previously known chiral doublet bands assigned the $\pi h_{11/2} \otimes \nu h_{11/2}$ configuration constitute a case of MχD bands in ^{128}La. It is the first example of MχD bands in odd-odd nuclei in the $A \approx 130$ mass region.

ACKNOWLEDGMENTS

This work is supported by the Jilin Scientific and Technological Development Program (Grant No. 20230101009JC); the National Natural Science Foundation of China (Grant No. 12175086, No. 11775098, No. U1867210, and No. 11405072); the Natural Science Foundation of Chongqing, China (Grant No. CSTB2022NSCQMSX0315); the Natural Science Foundation of Sichuan China (Grant No. 23NSFSC1051); and the Graduate Innovation Fund of Jilin University (Grant No. 2023CX051).

[1] S. Frauendorf and J. Meng, Nucl. Phys. A **617**, 131 (1997).
[2] J. Peng, J. Meng, and S. Q. Zhang, Phys. Rev. C **68**, 044324 (2003).
[3] T. Koike, K. Starosta, and I. Hamamoto, Phys. Rev. Lett. **93**, 172502 (2004).
[4] S. Y. Wang, S. Q. Zhang, B. Qi, and J. Meng, Phys. Rev. C **75**, 024309 (2007).
[5] S. Q. Zhang, B. Qi, S. Y. Wang, and J. Meng, Phys. Rev. C **75**, 044307 (2007).
[6] S. Y. Wang, S. Q. Zhang, B. Qi, J. Peng, J. M. Yao, and J. Meng, Phys. Rev. C **77**, 034314 (2008).
[7] B. Qi, S. Q. Zhang, J. Meng, S. Y. Wang, and S. Frauendorf, Phys. Lett. B **675**, 175 (2009).
[8] B. Qi, S. Q. Zhang, S. Y. Wang, J. Meng, and T. Koike, Phys. Rev. C **83**, 034303 (2011).
[9] V. I. Dimitrov, S. Frauendorf, and F. Dönau, Phys. Rev. Lett. **84**, 5732 (2000).
[10] P. Olbratowski, J. Dobaczewski, J. Dudek, and W. Płóciennik, Phys. Rev. Lett. **93**, 052501 (2004).
[11] P. W. Zhao, S. Q. Zhang, and J. Meng, Phys. Rev. C **92**, 034319 (2015).
[12] P. W. Zhao, Phys. Lett. B **773**, 1 (2017).
[13] Z. X. Ren, P. W. Zhao, and J. Meng, Phys. Rev. C **105**, L011301 (2022).
[14] S. Mukhopadhyay, D. Almehed, U. Garg, S. Frauendorf, T. Li, P. V. Madhusudhana Rao, X. Wang, S. S. Ghugre, M. P. Carpenter, S. Gros, A. Hecht, R. V. F. Janssens, F. G. Kondev, T. Lauritsen, D. Seweryniak, and S. Zhu, Phys. Rev. Lett. **99**, 172501 (2007).
[15] F. Q. Chen, Q. B. Chen, Y. A. Luo, J. Meng, and S. Q. Zhang, Phys. Rev. C **96**, 051303(R) (2017).
[16] F. Q. Chen, J. Meng, and S. Q. Zhang, Phys. Lett. B **785**, 211 (2018).
[17] S. Brant and C. M. Petrache, Phys. Rev. C **79**, 054326 (2009).

[18] H. G. Ganev and S. Brant, Phys. Rev. C **82**, 034328 (2010).
[19] Q. B. Chen, S. Q. Zhang, P. W. Zhao, R. V. Jolos, and J. Meng, Phys. Rev. C **87**, 024314 (2013).
[20] Q. B. Chen, S. Q. Zhang, P. W. Zhao, R. V. Jolos, and J. Meng, Phys. Rev. C **94**, 044301 (2016).
[21] Y. Zhang, B. Qi, and S. Q. Zhang, Sci. China: Phys., Mech. Astron. **64**, 122011 (2021).
[22] S. Frauendorf, Rev. Mod. Phys. **73**, 463 (2001).
[23] J. Meng and S. Q. Zhang, J. Phys. G: Nucl. Part. Phys. **37**, 064025 (2010).
[24] J. Meng, B. Qi, S. Q. Zhang, and S. Y. Wang, Mod. Phys. Lett. A **23**, 2560 (2008).
[25] B. W. Xiong and Y. Y. Wang, At. Data Nucl. Data Tables **125**, 193 (2019).
[26] C. Liu, S. Y. Wang, B. Qi, S. Wang, D. P. Sun, Z. Q. Li, R. A. Bark, P. Jones, J. J. Lawrie *et al.*, Phys. Rev. C **100**, 054309 (2019).
[27] R. A. Bark, E. O. Lieder, R. M. Lieder, E. A. Lawrie, J. J. Lawrie, S. P. Bvumbi, N. Y. Kheswa, S. S. Ntshangase, T. E. Madiba *et al.*, Int. J. Mod. Phys. E **23**, 1461001 (2014).
[28] J. Meng and P. W. Zhao, Phys. Scr. **91**, 053008 (2016).
[29] A. A. Raduta, Prog. Part. Nucl. Phys. **90**, 241 (2016).
[30] K. Starosta and T. Koike, Phys. Scr. **92**, 093002 (2017).
[31] C. Liu, S. Y. Wang, R. A. Bark, S. Q. Zhang, J. Meng, B. Qi, P. Jones, S. M. Wyngaardt, J. Zhao *et al.*, Phys. Rev. Lett. **116**, 112501 (2016).
[32] L. Mu, S. Y. Wang, C. Liu, B. Qi, R. A. Bark, J. Meng, S. Q. Zhang, P. Jones, S. M. Wyngaardt *et al.*, Phys. Lett. B **827**, 137006 (2022).
[33] I. Kuti, Q. B. Chen, J. Timar, D. Sohler, S. Q. Zhang, Z. H. Zhang, P. W. Zhao, J. Meng, K. Starosta *et al.*, Phys. Rev. Lett. **113**, 032501 (2014).
[34] J. Timár, P. Joshi, K. Starosta, V. I. Dimitrov, D. B. Fossan, J. Molnár, D. Sohler, R. Wadsworth, A. Algora *et al.*, Phys. Lett. B **598**, 178 (2004).
[35] J. A. Alcántara-Núñez, J. R. B. Oliveira, E. W. Cybulska, N. H. Medina, M. N. Rao, R. V. Ribas, M. A. Rizzutto, W. A. Seale, F. Falla-Sotelo, K. T. Wiedemann, V. I. Dimitrov, and S. Frauendorf, Phys. Rev. C **69**, 024317 (2004).
[36] B. Zhang, L. H. Zhu, H. B. Sun, C. Y. He, X. G. Wu, J. B. Lu, Y. J. Ma, X. Hao, Y. Zheng *et al.*, Chin. Phys. C **35**, 1009 (2011).
[37] B. Qi, H. Jia, N. B. Zhang, C. Liu, and S. Y. Wang, Phys. Rev. C **88**, 027302 (2013).
[38] S. Guo, C. M. Petrache, D. Mengoni, Y. H. Qiang, Y. P. Wang, Y. Y. Wang, J. Meng, Y. K. Wang, S. Q. Zhang *et al.*, Phys. Lett. B **807**, 135572 (2020).
[39] A. D. Ayangeakaa, U. Garg, M. D. Anthony, S. Frauendorf, J. T. Matta, B. K. Nayak, D. Patel, Q. B. Chen, S. Q. Zhang *et al.*, Phys. Rev. Lett. **110**, 172504 (2013).
[40] S. Zhu, U. Garg, B. K. Nayak, S. S. Ghugre, N. S. Pattabiraman, D. B. Fossan, T. Koike, K. Starosta, C. Vaman *et al.*, Phys. Rev. Lett. **91**, 132501 (2003).
[41] B. F. Lv, C. M. Petrache, Q. B. Chen, J. Meng, A. Astier, E. Dupont, P. Greenlees, H. Badran, T. Calverley *et al.*, Phys. Rev. C **100**, 024314 (2019).
[42] C. M. Petrache, B. F. Lv, A. Astier, E. Dupont, Y. K. Wang, S. Q. Zhang, P. W. Zhao, Z. X. Ren, J. Meng *et al.*, Phys. Rev. C **97**, 041304(R) (2018).
[43] B. F. Lv, C. M. Petrache, A. Astier, E. Dupont, A. Lopez-Martens, P. T. Greenlees, H. Badran, T. Calverley, D. M. Cox *et al.*, Phys. Rev. C **98**, 044304 (2018).
[44] C. M. Petrache, B. F. Lv, Q. B. Chen, J. Meng, A. Astier, E. Dupont, K. K. Zheng, P. T. Greenlees, H. Badran *et al.*, Eur. Phys. J. A **56**, 208 (2020).
[45] T. Roy, G. Mukherjee, Md. A. Asgar, S. Bhattacharyya, S. Bhattacharya, C. Bhattacharya, S. Bhattacharya, T. K. Ghosh, K. Banerjee *et al.*, Phys. Lett. B **782**, 768 (2018).
[46] K. Y. Ma, J. B. Lu, D. Yang, H. D. Wang, Y. Z. Liu, X. G. Wu, Y. Zheng, and C. Y. He, Phys. Rev. C **85**, 037301 (2012).
[47] M. J. Godfrey, Y. He, I. Jenkins, A. Kirwan, P. J. Nolan, D. J. Thornley, S. M. Mullins, and R. Wadsworth, J. Phys. G: Nucl. Part. Phys. **15**, 487 (1989).
[48] M. J. Godfrey, Y. He, I. Jenkins, A. Kirwan, P. J. Nolan, D. J. Thornley, S. M. Mullins, R. Wadsworth, and R. A. Wyss, J. Phys. G: Nucl. Part. Phys. **15**, 671 (1989).
[49] T. Hayakawa, J. Lu, J. Mukai, T. Saitoh, N. Hasimoto, T. Komatsubara, and K. Furuno, Z. Phys. A **352**, 241 (1995).
[50] K. Y. Ma, J. B. Lu, D. Yang, H. D. Wang, Y. Z. Liu, X. G. Wu, Y. Zheng, and C. Y. He, Phys. Rev. C **86**, 027301 (2012).
[51] K. Starosta, T. Koike, C. J. Chiara, D. B. Fossan, D. R. LaFosse, A. A. Hecht, C. W. Beausang, M. A. Caprio, J. R. Cooper *et al.*, Phys. Rev. Lett. **86**, 971 (2001).
[52] T. Koike, K. Starosta, C. J. Chiara, D. B. Fossan, and D. R. LaFosse, Phys. Rev. C **63**, 061304(R) (2001).
[53] G. Rainovski, E. S. Paul, H. J. Chantler, P. J. Nolan, D. G. Jenkins, R. Wadsworth, P. Raddon, A. Simons, D. B. Fossan *et al.*, Phys. Rev. C **68**, 024318 (2003).
[54] S. Y. Wang, Y. Liu, T. Komatsubara, Y. Ma, and Y. Zhang, Phys. Rev. C **74**, 017302 (2006).
[55] E. Grodner, J. Srebrny, A. A. Pasternak, I. Zalewska, T. Morek, Ch. Droste, J. Mierzejewski, M. Kowalczyk, J. Kownacki *et al.*, Phys. Rev. Lett. **97**, 172501 (2006).
[56] F. Dönau, Nucl. Phys. A **471**, 469 (1987).
[57] T. Koike, K. Starosta, C. J. Chiara, D. B. Fossan, and D. R. LaFosse, Phys. Rev. C **67**, 044319 (2003).
[58] T. Koike, K. Starosta, C. Vaman, T. Ahn, D. B. Fossan, R. M. Clark, M. Cromaz, I. Y. Lee, and A. O. Macchiavelli, in *Frontiers of Nuclear Structure*, edited by P. Fallon and R. Clark, AIP Conf. Proc. No. 656 (AIP, New York, 2003), p. 160.
[59] C. Vaman, D. B. Fossan, T. Koike, K. Starosta, I. Y. Lee, and A. O. Macchiavelli, Phys. Rev. Lett. **92**, 032501 (2004).
[60] H. J. Chantler, E. S. Paul, A. J. Boston, M. P. Carpenter, R. Charity, C. J. Chiara, P. T. W. Choy, C. N. Davids, M. Devlin *et al.*, Phys. Rev. C **66**, 014311 (2002).
[61] K. Selvakumar, A. K. Singh, C. Ghosh, P. Singh, A. Goswami, R. Raut, A. Mukherjee, U. Datta, P. Datta *et al.*, Phys. Rev. C **92**, 064307 (2015).
[62] R. Kumar, A. Kumar, S. K. Chamoli, K. Singh, M. Sharma, D. Mehta, N. Singh, S. S. Ghugre, N. S. Pattabiraman *et al.*, Phys. Rev. C **72**, 044319 (2005).